Turkish Journal of Electrical Engineering & Computer Sciences

http://journals.tubitak.gov.tr/elektrik/

Research Article

Turk J Elec Eng & Comp Sci
(2017) 25: 3904 – 3919

doi:10.3906/elk-1703-147

Concurrent optimal design of TCSC and PSS using symbiotic organisms search algorithm

Muwaffaq ALOMOUSH*
Department of Electrical Power Engineering, Hijjawi Faculty for Engineering Technology, Yarmouk University, Irbid, Jordan

Received: 12.03.2017 • **Accepted/Published Online:** 01.06.2017 • **Final Version:** 05.10.2017

Abstract: The symbiotic organisms search (SOS), which has been recently introduced, is a robust powerful metaheuristic global optimizer. This nature-inspired algorithm imitates the symbiotic interaction strategies in an ecosystem exercised by organisms involved in interrelationships to survive and reproduce. One of the main beneficial features of the SOS in contrast to many other competent metaheuristic algorithms is that the algorithm does not need any specific algorithm parameters or tuning process. This paper applies the SOS algorithm to simultaneously design optimal controllers of a power system equipped with both a power system stabilizer (PSS) and a thyristor-controlled series compensator (TCSC). The algorithm of SOS is utilized to concurrently tune the variables of controllers for both the PSS and TCSC in the nonlinear optimization process. Simulation results reveal that the optimal SOS-based coordinated controllers can significantly stabilize the system and efficiently damp oscillations under severe disturbances. Results will also show that the optimal controllers obtained perform slightly better than the optimal controllers obtained using the two commonly used global optimization solvers, the genetic algorithm (GA) and particle swarm optimization.

Key words: Global optimization, optimal controllers, power system control, power system stabilizer, stability, symbiotic organisms search, thyristor-controlled series compensator

1. Introduction

Several devices and control methods have been introduced to enhance damping in power systems in order to maintain a reliable operation of the system [1–3]. Among the devices are the power system stabilizer (PSS) and thyristor-controlled series compensator (TCSC).

Power system stability, oscillation problems, and PSS design have received increased consideration over the last five decades [2–12]. Parameters of classical PSSs are commonly achieved in the frequency domain using the phase compensation technique, realized using lead-lag compensators whose control parameters are usually obtained depending on linear modeling of the power system [1–3].

Many control practices have been introduced to design PSSs with an enhanced performance. In addition to classical control schemes [1 – 3], other alternatives include artificial intelligence techniques [4,5], global optimization algorithms [6 – 9], robust control methods [10], and linear and nonlinear control methods [11]. Hybrid control methods have received more emphasis recently in designing PSSs [12].

The TCSC is effective to enhance power system stability, dampen system oscillations, mitigate the

*Correspondence: ma@yu.edu.jo

subsynchronous resonance, control steady-state power flow, and improve the economic value of transmission system [13–18].

Modeling and simulation of a single-machine infinite-bus (SMIB) power system equipped with a TCSC and optimal tuning of the TCSC controller in this system were presented in many research papers in the last two decades [14 − 18]. To improve overall system performance, some research papers proposed coordinated operations of the PSS and FACTS controllers to boost damping achievements of a power system [19–30]. In this literature, artificial techniques such as the GA, PSO, and simulated annealing (SA) algorithms were used to tune TCSC parameters or to design coordinated controllers of the TCSC and the PSS [17 − 30]. However, most of the work was based on linearized power system models.

The work in [22] presented modeling and simulation of a SMIB system equipped with PSS and TCSC controllers using MATLAB programming. This work proposed lead-lag and proportional-integral controller structures for the TCSC, which were tested under different loading conditions and a symmetrical three-phase short circuit fault. The work presented in [23] applied the teaching–learning-based optimization algorithm to design a coordinated proportional-integral (PI) controller-based PSS for SMIB power systems equipped with TCSCs, which was tested under various loading conditions. The study presented in [24] investigated the effectiveness of the damping function of TCSC in a SMIB system by applying a two-stage lead-lag PPS, linear optimal control-based power oscillation damping, and a new controller design scheme based on modal optimal control, where the GA is used to design the PSS controller parameter and weighting matrix of the linear and modal optimal controls, and the stability of the system with the proposed controllers was investigated using small load disturbances. In [25], the researchers developed a modified PSO for coordination of a PSS and a TCSC controller to enhance the power system's small-signal stability. The proposed approach simultaneously used eigenvalue-based and time-domain simulation-based objective functions to improve the optimization convergence rate. The bacterial foraging algorithm was used in [26] to design a PSS and TCSC as a damping controller in a SMIB system for damping low-frequency oscillations under different loading conditions. The problem of robustly PSS- and TCSC-based damping controllers was formulated as an optimization problem according to the eigenvalue-based objective function comprising the damping factor and the damping ratio of the undamped electromechanical modes. The work in [27] presented a design of state-feedback controllers for a PSS and TCSC whose parameters were optimized based on PSO to analyze their effects on the stability of a SMIB system and to damp the low-frequency oscillations. The proposed controllers were explained using eigenvalues analysis and performance indices. In [28] an improved harmony search algorithm was proposed for coordinated design of the PSS and TCSC to effectively damp interarea oscillations. To demonstrate the effectiveness of the proposed technique, the results obtained were compared to the results obtained using other four optimization algorithms. The research presented in [29] introduced the bacterial swarm optimization for simultaneous coordinated design of power PSSs and TCSCs in a multimachine power system over a wide range of loading conditions. The algorithm was employed to search for optimal controllers parameters. The study presented in [30] proposed a multiobjective genetic algorithm employing the Pareto method type of selection to solve the optimization problem of a SMIB system equipped with PSS and TCSC controllers. The conflicting objective functions used in this study were the synchronizing and damping torques.

SOS is one of the recent heuristic algorithms, which was introduced in 2014 [31]. It imitates the symbiotic interaction strategies implemented by organisms involved in interrelationships in an ecosystem to survive and reproduce. This algorithm is superior to other algorithms in the sense that it does not need any specific algorithm parameters or tuning processes.

In 2016 and 2017, the SOS optimization algorithm was successfully applied to solve power engineering optimization problems and compared with other metaheuristic methods [32 − 35]. The results presented in these studies showed that the algorithm had good convergence and produced better results than some other metaheuristic optimization methods. In [32] the SOS was used to show the superiority of the algorithm to solve the classical economic dispatch problem, which has either a smooth fuel cost function or nonconvex and discontinuous fuel cost function considering some practical constraints. In [33] the SOS algorithm was proposed to optimize the power generation strategy while satisfying some operational constraints in the short-term hydrothermal generation scheduling problem. The research presented in [34] applied the SOS algorithm to solve the multiobjective economic emission load dispatch problem for thermal generators to minimize both total operating costs and emission levels, while satisfying equality constraints and limits. In the study presented in [35], the SOS algorithm was proposed to solve the dynamic economic dispatch problem with valve-point effects considering some practical constraints and the obtained results were compared with other some metaheuristic methods.

In this paper we use the SOS for concurrent design of optimal controllers of the PSS and TCSC to improve transient and steady-state responses and stability of a nonlinear SMIB system. The achieved SOS-based optimal controllers are investigated on three different typical disturbances. The results are compared with the results attained using two well-recognized and trusty global optimization algorithms, which are the GA and PSO [37,38]. The paper will verify that the SOS algorithm leads to a better global solution of the optimization problem of the system under study with small computational time. The results presented in this paper will reveal that utilizing the coordinated optimal SOS-based controllers of the TCSC and PSS is robust and effective in damping the electromechanical oscillations of the speed deviation, rotational speed, and electromagnetic torque under severe disturbances. Moreover, it will indicate that the SOS-based optimal controllers show better performance than the other two algorithms in treating different perturbations. Results presented in this paper will verify that the computation time associated with the SOS algorithm is much smaller than the computational times of the other two optimization algorithms.

2. Model of the system under study

Figure 1 depicts the SMIB power system under study, which comprises a combination of a generating unit, a transformer, three transmission lines, a TCSC, and the equivalent circuit of a large power system to which the combination is connected. Thevenin's equivalent impedance (Z_{TH}) and the voltage (V_b) of the large power system is employed to represent the system connected to the combination. The TCSC is inserted in the single transmission line (T.L.3) as this line has the largest reactance in the system to guarantee the largest possible flexibility to control the reactance of the line while the net reactance of the line is kept inductive. This location has been chosen based on simulation results obtained from the three possible locations of the TCSC.

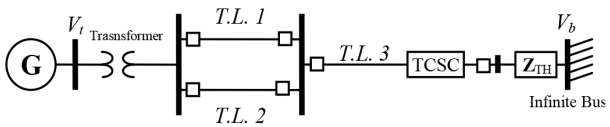

Figure 1. Diagram of SMIB system including TCSC.

2.1. TCSC

The circuit shown in Figure 2a represents a TCSC inserted in a line connecting buses i and j, where z_{ij} refers to the series impedance of the transmission line [13−21]. The equivalent reactance of the TCSC is depicted as a function of the firing angle (α) as shown in Figure 2b.

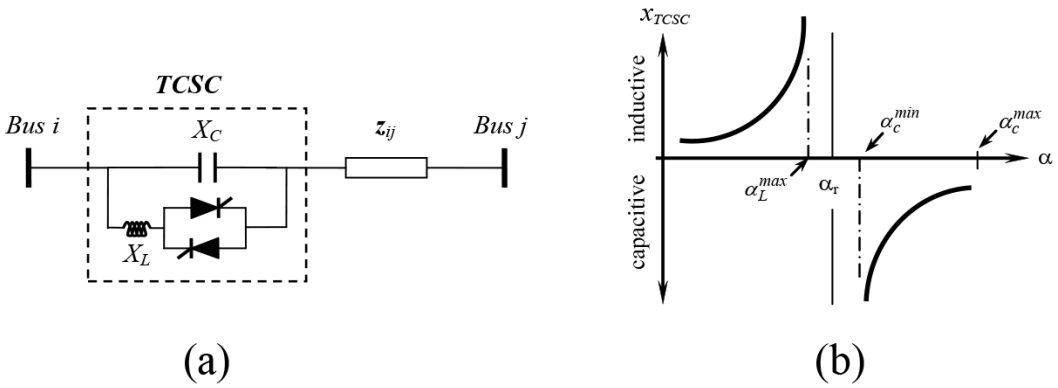

Figure 2. (a) A line equipped with TCSC, (b) equivalent reactance of TCSC.

The TCSC comprises a capacitor bank with a reactance of X_C connected in a shunt thyristor-controlled inductor with a reactance of X_L. The TCSC is seen by the transmission system as an equivalent controllable reactance (x_{TCSC}), which is a function of α. A resonance situation that takes place for the parallel combination of inductance-capacitance at α_r should be bypassed. As presented in Figure 2b, a margin of safety for the resonance situation is maintained by limiting α to be $\alpha \geq \alpha_r + \Delta\alpha$ in the capacitive region and $\alpha \leq \alpha_r - \Delta\alpha$ in the inductive region [13−18].

The operating boundaries of x_{TCSC} are decided based on the limits of α. Consequently, the limits of x_{TCSC} are expressed as:

$$X_{TCSC}^{\min} \leq x_{TCSC} \leq X_{TCSC}^{\max}. \tag{1}$$

In the inductive region, limits on α are expressed as:

$$\alpha_L^{\min} \ \leq \ \alpha \ \leq \ \alpha_L^{\max}; \ \alpha_L^{\min} = \pi/2. \tag{2}$$

In the capacitive region, limits on α are expressed as:

$$\alpha_C^{\min} \ \leq \ \alpha \ \leq \ \alpha_C^{\max}; \ \alpha_C^{\max} = \pi. \tag{3}$$

If $\sigma = \pi - \alpha$, x_{TCSC} as a function of σ is given by [17,18]:

$$x_{TCSC}(\sigma) = -X_C + k_1(2\sigma + \sin(2\sigma)) \ - k_2(\cos^2\sigma)(\varpi\tan(\varpi\sigma) - \tan\sigma)), \tag{4}$$

Where

$$k_1 = \frac{X_C + X_{LC}}{\pi}, \quad k_2 = \frac{4X_{LC}^2}{\pi X_L}, \quad X_{LC} = \frac{X_C X_L}{X_C - X_L}, \quad \varpi = \sqrt{\frac{X_C}{X_L}}. \tag{5}$$

In this paper the commonly used lead-lag structure as a TCSC controller has been utilized. The block diagram representation of the lead-lag controller and the TCSC is illustrated in Figure 3. The TCSC controller can be represented by the following transfer function ($G_{TCSC}(s)$):

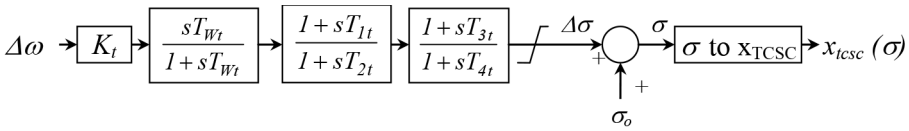

Figure 3. Block diagram for TCSC and its controller.

$$G_{TCSC}(s) = \frac{\Delta\sigma(s)}{\Delta\omega(s)} = K_t \frac{sT_{wt}}{1+sT_{wt}} \frac{1+sT_{1t}}{1+sT_{2t}} \frac{1+sT_{3t}}{1+sT_{4t}} \quad , \tag{6}$$

where K_t, T_{Wt}, and T_{1t}-T_{4t} are the TCSC controller stabilizing gain, washout time constant, and phase lead-lag time constants, respectively. The reactance introduced by the TCSC as a function of σ is given by Eq. (4).

2.2. SMIB system

The system dynamics can be expressed by a group of differential equations in the variables $\delta(t)$, $S_m(t)$, $E'_q(t)$, $E'_d(t)$, and $E_{fd}(t)$ as follows [1]:

$$\frac{d}{dt}(\delta(t)) = 2\pi f(S_m - S_{mo}) \quad , \tag{7}$$

$$\frac{d}{dt}(S_m(t)) = \frac{1}{2H}(-D(S_m - S_{mo}) + T_m - T_e), \tag{8}$$

$$\frac{d}{dt}(E'_q(t)) = \frac{1}{T'_{do}}[-E'_q(t) + E_{fd}(t) + (x_d - x'_d)i_d], \tag{9}$$

$$\frac{d}{dt}(E'_d(t)) = \frac{1}{T'_{qo}}[-E'_d(t) + (x_q - x'_q)i_q], \tag{10}$$

$$\frac{d}{dt}(E_{fd}(t)) = \frac{1}{T_A}[K_A(V_{ref} - V_t - u_{PSS}) - E_{fd}(t)], \tag{11}$$

where

$$v_q(t) = E'_q(t) - x'_d i_d(t), \quad v_d(t) = E'_d(t) + x'_q i_q(t); \quad V_t = \sqrt{v_d^2 + v_q^2}, \tag{12}$$

$$i_d(t) = \frac{E'_q(t) - V_b\cos(\delta(t))}{x_e + x'_d}, \quad i_q(t) = \frac{V_b\sin(\delta(t)) - E'_d(t)}{x_e + x'_q}, \tag{13}$$

$$T_e(t) = E'_d(t)i_d(t) + E'_q(t)i_q(t) + (x'_q - x'_d)i_d(t)i_q(t)], \tag{14}$$

$$x_e = x_T + x_L - x_{t\,\mathrm{csc}} + x_{TH}; \quad x_L = \frac{x_{L1}x_{L2}}{x_{L1} + x_{L2}} + x_{L3}, \tag{15}$$

and:

S_m, S_{mo}	Generator slip and initial slip, p.u.
δ, D	Rotor angle in radians and damping torque coefficient of generator, p.u.
E_{fd}	Equivalent field (excitation) voltage, p.u.
E'_q	Transient voltage in the q-axis of the generator, p.u.
i_d, i_q	d-axis and q-axis components of armature current, p.u.
K_A, T_A	Exciter gain and exciter time constant in s, respectively.
T_e, T_m	Electrical and mechanical torques, respectively, p.u.
T'_{do}	Transient time constant of d-axis open circuit, s.
u_{pss}	Output signal of the PSS, p.u.
v_d, v_q	d-axis and q-axis of the generator terminal voltages, respectively, p.u.
V_t, H	Terminal voltage in p.u. and inertia constant in s of the generator.
x_d, x_q	d-axis and q-axis of the generator synchronous reactances, respectively, p.u.
x'_d, x'_q	d-axis and q-axis of the transient reactances of the generator, respectively, p.u.
x_e	Equivalent impedance of the system external to the machine terminals, p.u.
X_L, X_T	Reactances of the lines and the transformer, respectively, p.u.
X_{TH}	Thevenin's equivalent reactance of the transmission network external to the TCSC-inserted line, p.u.

2.3. PSS

The PSS basically controls the generator's excitation by adding damping to rotor oscillations by using one or more auxiliary stabilizing signals [1–3]. A standard conventional lead-lag PSS encompasses three blocks for phase compensation, signal washout, and gain. As the function of a PSS is to offer a component of damping torque, the speed deviation ($\Delta\omega$) represents a suitable input signal for the PSS. The block diagram of the lead-lag PSS is illustrated in Figure 4, and the corresponding transfer function is given by:

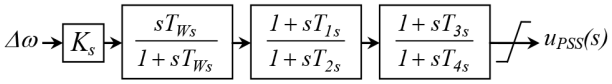

Figure 4. Block diagram for lead-lag PSS.

$$G_{PSS}(s) = \frac{u_{PSS}(s)}{\Delta\omega(s)} = K_s \frac{sT_{ws}}{1+sT_{ws}} \frac{1+sT_{1s}}{1+sT_{2s}} \frac{1+sT_{3s}}{1+sT_{4s}}. \tag{16}$$

In the PSS, K_s, T_{Ws}, and T_{1s}–T_{4s} are the PSS stabilizing gain, washout time constant, and phase lead-lag time constants, respectively. The parameters of the lead-lag PSS are required to be tuned optimally to obtain the best achievement of the system [1,2].

2.4. Design of optimal controllers

The parameters associated with the PSS and TCSC to be optimally adjusted are the time constants ($T_{1s}-T_{4s}$ and $T_{1t}-T_{4t}$) and stabilizing gains (K_s and K_t). Washout time constants $T_{Ws} = T_{Wt} = 10$ are used in this work. The integral of the time-weighted absolute error (ITAE) performance measure that uses speed deviation has been utilized in this paper, which is mathematically expressed as [36]:

$$ITAE = \int_0^{t_s} t|\Delta\omega(t)|dt, \tag{17}$$

where t_s is the simulation time, which is 10 s in this current paper. The optimal settings of controller gains are attained as the results of the constrained optimization of the ITAE performance measure (the objective

function). The optimization problem can be formulated mathematically as follows:

Minimize

$$ITAE\left(K_{Ps}, T_{1s}, T_{2s}, T_{3s}, T_{4s}, K_t, T_{1t}, T_{2t}, T_{3t}, T_{4t}\right) \tag{18}$$

subject to

$$K_s^{\min} \le K_s \le K_s^{\max}, \quad K_t^{\min} \le K_t \le K_t^{\max}, \quad T_{is}^{\min} \le T_{is} \le T_{is}^{\max}, \quad T_{it}^{\min} \le T_{it} \le T_{it}^{\max}; \quad i = 1, 2, 3, 4.$$

In this paper, MATLAB and Simulink environments are used to solve the above optimization problem using SOS [31] and both GA [37] and PSO algorithms [38].

3. Symbiotic organisms search

Symbiosis describes any association between unlike organisms (species), which can defined as the interrelationship between two or more different organisms living together in the ecological system with some form of feeding relationship involved. The SOS algorithm imitates the three symbiotic interactions within an interrelationship that involve a pair of organisms seeking the fittest organism. The SOS technique uses in its iterative process a population of hopeful solutions to best regions in the search space in the procedure seeking the global optimal solution [31].

The SOS starts with a starting ecosystem. In this ecosystem, a set of organisms is created randomly in the search space. Each organism among them serves as one possible solution to the optimization problem. In the ecosystem, each organism is accompanied by a specific fitness value, which indicates the degree of closeness to the desired objective. The SOS algorithm applies a sequence of operations in each iteration to current solutions to create revised solutions for the following iteration. The new solution in SOS is generated by simulating the coaction between two organisms in the biological ecosystem [31].

The procedures in the SOS involve three phases that mimic the interaction model of a real biological ecosystem, which are described in the following subsections.

3.1. Mutualism phase

In the SOS, X_i is an organism corresponding to the ith member of the ecosystem. Another organism, X_j, is then randomly picked from the ecosystem to interact with X_i. The two organisms interact in a mutualistic relationship aiming at increasing the mutual survival level in the ecosystem. New possible solutions for X_i and X_j are evaluated depending on the mutualistic symbiosis between organisms X_i and X_j, which are modeled by [31]:

$$X_i^{new} = X_i + r(0,1)\ (X_{best} - V_m\, BF_1); \quad V_m = (X_i + X_j)/2, \tag{19}$$

$$X_j^{new} = X_j + r(0,1)\ (X_{best} - V_m\, BF_2); \quad V_m = (X_i + X_j)/2, \tag{20}$$

where $r(0,1)$ is a random-number vector and V_m is the mutual vector that represents the relationship characteristics between organisms X_i and X_i. The benefit factors (BF_1 and BF_2) in Eqs. (19) and (20) express the level of benefit of every organism, which indicate if an organism partly or fully benefits from the engaged interaction, which are determined randomly as either 1 or 2 [31]. The $(X_{best} - V_m\, BF_1)$ and $(X_{best} - V_m\, BF_2)$ parts in Eqs. (20) and (21) indicate the mutualistic effort to accomplish their target in improving their survival advantage [31]. The best organism (X_{best}) represents the maximum degree of adaptation. The SOS uses

X_{best} (global solution) to simulate the maximum degree of adaptation as the destination point for the fitness increase of the two organisms. Lastly, organisms are revised only if their recent fitness is greater than their fitness before interaction [31].

3.1.1. Commensalism phase

In this second phase, organism X_j is randomly picked from the ecosystem to engage in interaction with another organism, X_i, that seeks advantage from the interaction, while the other counterpart organism X_j neither suffers nor benefits. The new candidate solution of X_i (or X_i^{new}) is evaluated based on the following commensal symbiotic interrelation between organisms X_i and X_j [31]:

$$X_i^{new} = X_i + r(-1,1)\ (X_{best} - X_j). \tag{21}$$

After this step, evaluation of the fitness value of the recent organism takes place, and organism X_i is revised only if its new fitness value is found better than its fitness before interaction. Note that $(X_{best} - X_j)$ in Eq. (21) indicates the beneficial advantage provided by organism X_j to help organism X_i increase its survival advantage in the ecosystem to the maximum degree for the present organism (represented by X_{best}) [31].

3.1.2. Parasitism phase

In the SOS, organism X_i is given the task of creating a factitious parasite called 'parasite vector' (V_p) from itself, which is generated in the search space by replicating organism X_i and then adjusting the randomly chosen dimensions utilizing a random number. Organism X_j is randomly picked from the ecosystem and plays as a host to V_p. The vector V_p attempts to replace X_j as follows: the two organisms are estimated to measure their fitness values. If V_p has a better fitness value, it eliminates organism X_j and takes its location in the ecosystem. On the contrary, if the fitness value of X_j is better than the fitness value of V_p, X_j is protected against the parasite and V_p will disappear from that ecosystem [31].

Figure 5 shows the flowchart of the SOS algorithm. The flowcharts of the GA and PSO and the associated details are given in [18,21,39].

4. Simulation results

This section discloses simulation results of the SMIB system using the SOS-based coordinated optimal adjusting of PSS and TCSC controllers. System data used in this paper are given in Table 1. Lower and upper limits of the PSS and TCSC controller parameters are presented in Table 2.

Table 1. System data of the SMIB system.

Machine	$x_d = 1.790, x_q = 1.66, \quad x'_d = 0.355, \quad T'_{do} = 7.9, \quad T'_{qo} = 0.410, \quad D = 2, \quad H = 3.77$
Transmission line	$x_{L1} = 0.2, \quad x_{L2} = 0.2, \quad x_{L3} = 0.5$
Transformer	$x_T = 0.1$
Thevenin's equivalent	$x_{TH} = 0.10, \quad V_b = 1$
Exciter	$K_A = 400, \quad T_A = 0.025, \quad -1 \leq E_{fd} \leq 1$
TCSC	$X_C = 0.30, \quad X_P = 0.25X_C, \quad k = 2, \quad T_{t\,\mathrm{csc}} = 0.015, \quad K_{t\,\mathrm{csc}} = 0.5$

To indicate the effectiveness of the SOS to optimally adjust TCSC and PSS control parameters, the results will be compared with the results obtained using the GA [37] and PSO [38]. The GA and PSO are selected

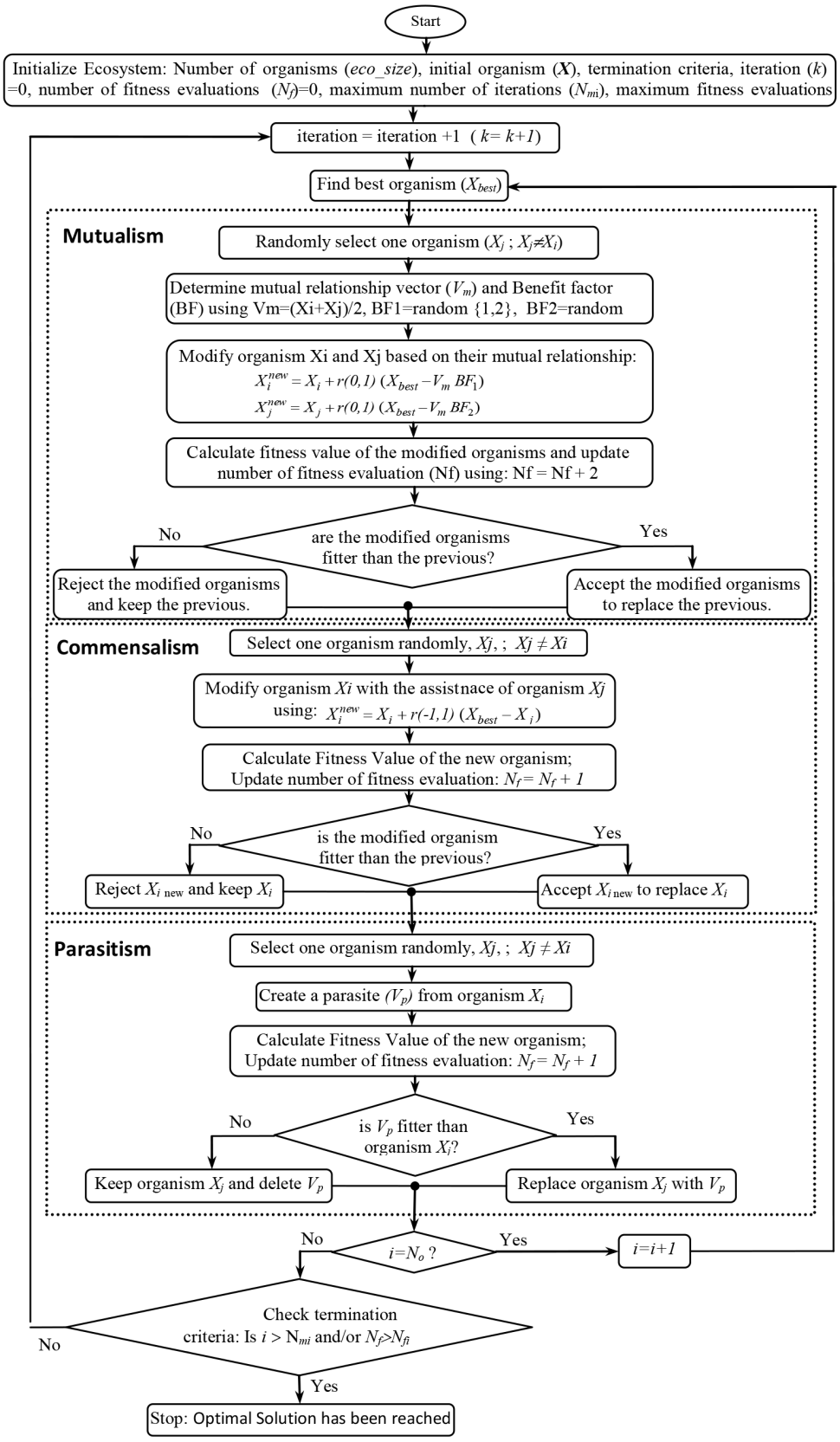

Figure 5. Flowchart of SOS algorithm.

Table 2. Lower and upper limits of controller parameters.

Parameters	Minimum limit	Maximum limit
K_s,K_t	0.10	100
T_{1s}, T_{2s}, T_{3s}, T_{4s}	0.01	2.0
T_{1t}, T_{2t}, T_{3t}, T_{4t}	0.01	2.0

in this paper for comparisons as they have become very common for solving optimization problems to find near-optimal global solutions. The user-provided parameters for the three optimization algorithms employed in this paper are given in Table 3.

Table 3. User parameters of optimization algorithms.

Algorithm	Parameters	Values
SOS	Ecosystem/population size	50
	Maximum number of function evaluations	5000
GA	Population size	250
	Number of generations	250
PSO	Maximum number of iterations	50
	Acceleration coefficients (C_1, C_2)	1.02, 0.12
	Inertia weight (W)	0.0004

In the simulations, three types of perturbations are used to examine the system, which are:

1. A three-phase 5-cycle short-circuit fault at the terminals of generator at $t = 2$ s.
2. A sudden increase of 10% in the input mechanical power ($\Delta T_m = 0.2$) at $t = 2$ s.
3. A permanent outage of one of the two parallel transmission lines at $t = 2$ s.

For each type of disturbance, we consider the following four typical scenarios:

(a) NOC: System with no PSS and TCSC,

(b) SOSC: System equipped with both PSS and TCSC controllers whose optimal parameters are determined using SOS,

(c) GAC: System equipped with both PSS and TCSC controllers whose optimal parameters are determined using GA, and

(d) PSO: System equipped with both PSS and TCSC controllers whose optimal parameters are determined using PSO.

As the three-phase 5-cycle short-circuit fault has the most severe impact on system behavior, the controllers are designed based on this disturbance.

4.1. Three-phase fault

By solving the optimization problem under the short-circuit fault at the generator terminals using the SOS, GA, and PSO, the optimal controller parameters for the system under study and computational time are obtained and summarized in Table 4. As can be noticed from the results presented in Table 4, the values of ITAE associated with the SOS-based optimal controllers are slightly smaller (better) than those obtained using the GA-based and PSO-based optimal controllers. This fact will be reflected in the following response figures. This table also shows that the computational time of the SOS algorithm is the smallest, which is considerably smaller than the computational burden of the other two optimization algorithms.

Table 4. Optimal TCSC and PSS controller parameters and computational time.

	Optimization algorithm		
	GA	PSO	SOS
ITAE	66.8×10^{-4}	67.0×10^{-4}	63.6×10^{-4}
Computational time (s)	144.699737	538.863344	68.871554
K_t	96.19019	77.38869	97.06685
T_{1t}	1.31065	0.58956	2.00000
T_{2t}	0.85705	0.24485	1.27100
T_{3t}	1.89912	1.90459	1.85122
T_{4t}	0.72567	0.52470	0.58240
K_s	7.90551	38.44753	45.16601
T_{1s}	0.75339	1.97184	0.01000
T_{2s}	1.43138	1.52590	1.41250
T_{3s}	0.28843	0.01211	2.00000
T_{4s}	1.21053	0.77755	0.52526

The responses of electrical torque (T_e), slip (S_m), reactance of the TCSC ($x_{t\,\mathrm{csc}}$), and rotor angle (δ) of the SMIB system following the three-phase fault for the four scenarios are shown in Figures 6–9. As the responses in these figures depict, the SMIB system without controllers witnesses unsatisfactory long-persisting oscillations with considerable settling time and large overshoots, but the SMIB system with optimal controllers exhibits satisfactorily stabilized oscillations with greatly reduced settling time and overshoots. The results also reveal that optimal SOS-based TCSC and PSS controllers give slightly better results compared to those of the GA-based and PSO-based optimal controllers. This was clear from the optimal values of the objective function given in Table 4.

4.2. Transmission line outage

The responses of the SMIB system variables following the outage of the line are shown in Figures 10-12, which present the responses of the electrical torque, the slip, and the rotor angle, respectively. Even though the impact of the line outage on the SMIB is less severe than the short-circuit fault discussed previously, the responses under the current disturbance still reveal undesired poorly stabilized performance of the SMIB system.

As the responses in these figures show, the SMIB system with coordinated optimal controllers also exhibits satisfactorily stabilized oscillations with greatly reduced settling time and overshoots. The results again demonstrate that optimal SOS-based controllers give slightly better results compared to the GA-based and PSO-based optimal controllers.

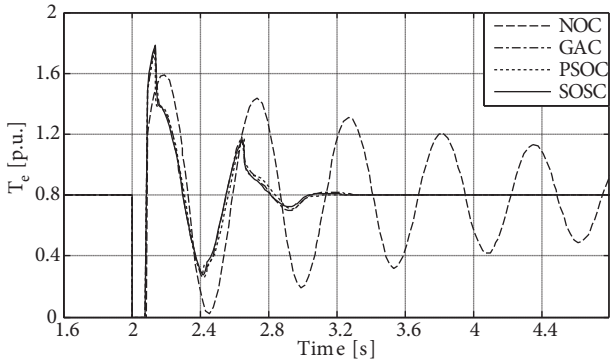

Figure 6. Electrical torque following the three-phase short-circuit fault.

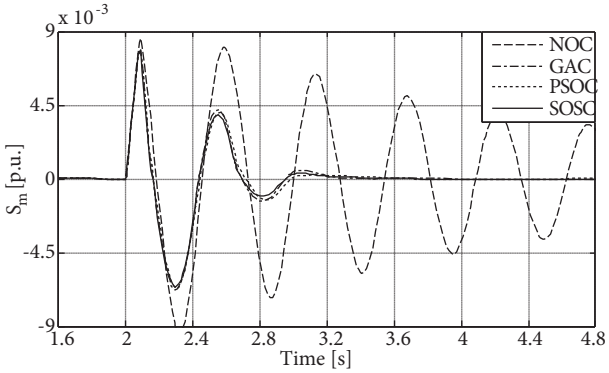

Figure 7. Slip following the three-phase short-circuit fault.

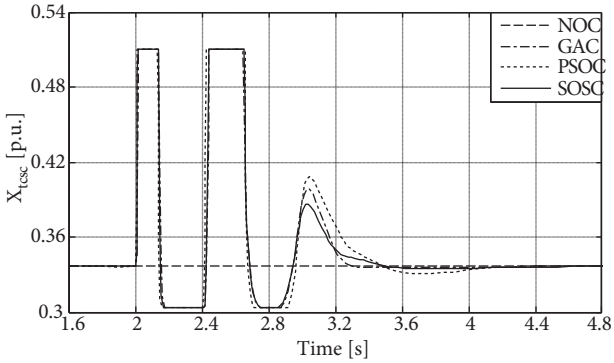

Figure 8. Reactance of TCSC following the three-phase short-circuit fault.

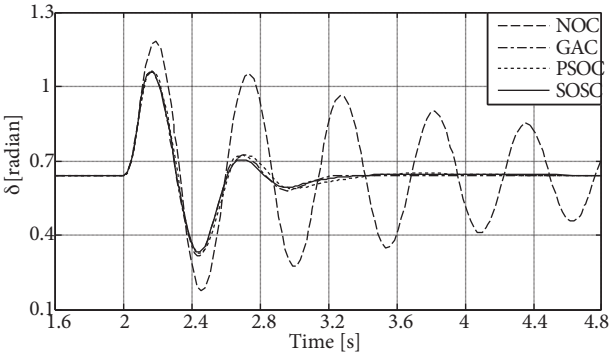

Figure 9. Rotor angle following the three-phase short-circuit fault.

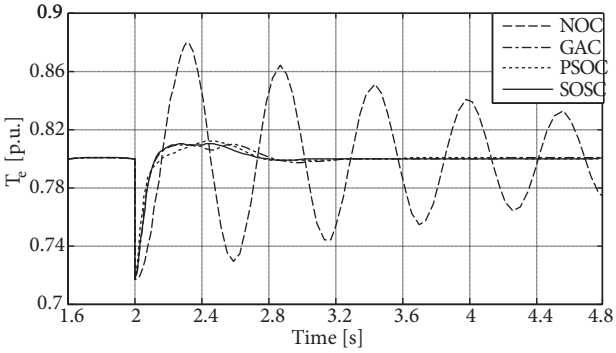

Figure 10. Electrical torque following the outage of line 3.

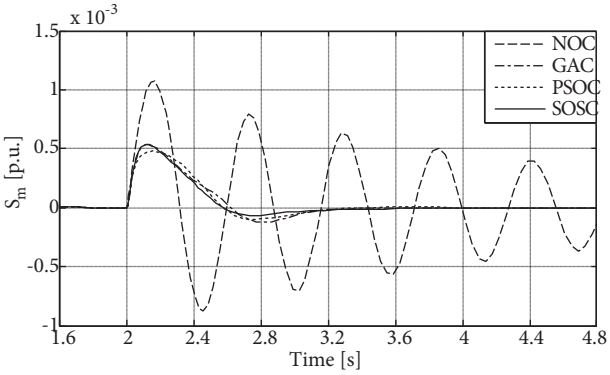

Figure 11. Slip following the outage of line 3.

4.3. Mechanical torque disturbance

Figures 13-15 show, respectively, changes in the system variables T_e, S_m, and δ following a sudden increase of 10% in T_m. It is clear from these figures that the impact of the mechanical torque disturbance has less severity than the short-circuit fault and nearly the same severity as the line outage. The current disturbance still reveals the undesired poorly stabilized performance of SMIB system. The same conclusions are drawn for this disturbance as in the case of the previous two disturbances. Again, as the responses in these figures show, the SMIB system with coordinated optimal controllers also exhibits satisfactorily stabilized oscillations with

greatly reduced settling time and overshoots. The results again demonstrate that optimal SOS-based controllers give slightly better results compared to the GA-based and PSO-based optimal controllers.

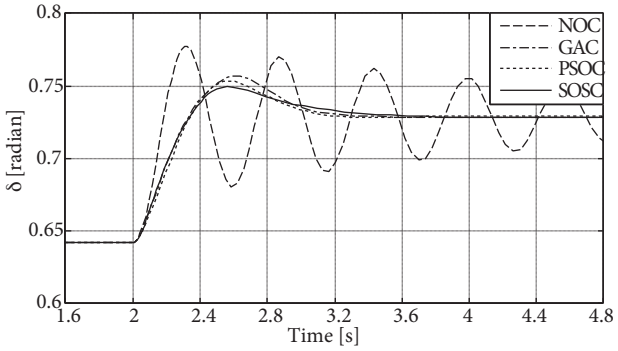

Figure 12. Rotor angle following the outage of line 3.

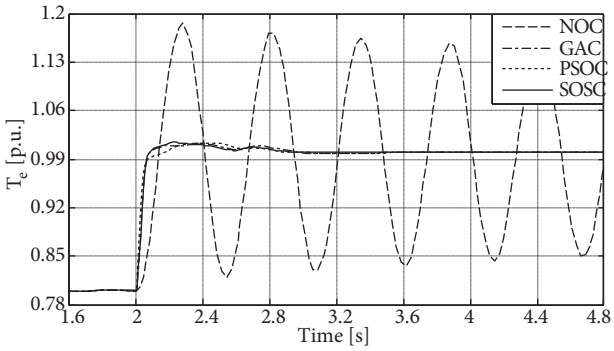

Figure 13. Electrical torque following a sudden increase of 10% in T_m.

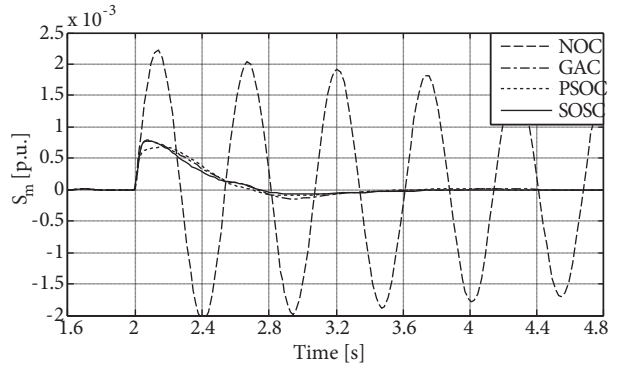

Figure 14. Slip following a sudden increase of 10% in T_m.

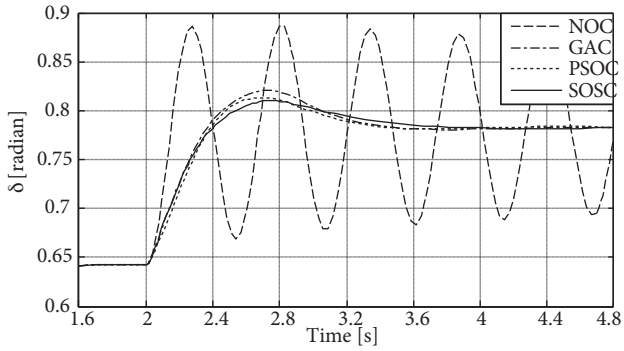

Figure 15. Rotor angle following a sudden increase of 10% in T_m.

The results presented in this section show that TCSC is a powerful device to improve both steady-state and transient responses of the SMIB system under different types of system disturbances. Measured by the ITAE optimal values, the results also show that tuning the TCSC and PSS using the SOS algorithm gives slightly better results compared to tuning using both the GA and PSO.

5. Discussion of results

Based on the results, figures, and comparisons carried out in the previous section, the following observations are made:

(1) Under all types of disturbances, the power system without controllers witnesses poor sustained oscillations with large settling time and large overshoots.

(2) The most severe disturbance is the short-circuit fault. Even though the impact of the line outage and change in mechanical power on the SMIB are less severe than the short-circuit fault, the same conclusions are drawn for the last two disturbances as in the case of the first disturbance, where the responses under the last two disturbances without controllers still reveal the undesired poorly stabilized performance of SMIB system.

(3) Utilizing the coordinated optimal SOS-based controllers of the TCSC and PSS offers the power system acceptably stabilized oscillations with greatly reduced settling time and overshoots. The optimal controllers are very effective in damping the electromechanical oscillations of the speed deviation, rotational speed, electromagnetic torque, and certainly the rest of variables presented in Eqs. (7)−(15).

(4) All of the previous results in the last section show that the TCSC, whose controllers are tuned using the SOS, is a powerful device to improve both transient and steady-state behavior of the SMIB system under different types of system disturbances. The improvement associated with the SOS are due to the fact that the algorithm of the SOS leads to a better global or near-global solution of the optimization problem.

(5) The results of comparisons in the last section show that tuning the parameters of the TCSC and PSS using the SOS algorithm gives better results compared to the results obtained using the GA and PSO. This is also made obvious by comparing the values of the objective functions associated with the SOS, GA, and PSO algorithms at the optimal solution (see first row in Table 4).

(6) The SOS-based optimally tuned parameters of the TCSC and PSS under severe disturbances are robust and effective, and they have enhanced different responses of the system and show better performance than the other two algorithms in treating different perturbations.

(7) As the second row in Table 4 shows, the computational time associated with the SOS algorithm to reach a better near-global solution is much smaller than the computational times of the other two optimization algorithms.

6. Conclusions

The work in this paper presented the coordinated optimal design of the PSS and TCSC in a SMIB system based on the SOS algorithm, which is capable of attaining a completive and better near-global optimal solution under different disturbance conditions. To indicate the effectiveness of the SOS to adjust the control parameters of the TCSC and PSS, the results were compared with the results obtained using the two traditionally used global optimization algorithms, the GA and PSO. Simulation results have shown that the optimal coordinated design of the PSS and TCSCS obtained using the SOS has significantly improved the stability and damping of the system and provides better results compared to both the GA and PSO. Utilizing the coordinated optimal SOS-based controllers of the TCSC and PSS offered the power system acceptably stabilized oscillations with reduced settling time and overshoots. The optimal controllers were very effective in damping the electromechanical oscillations of the speed deviation, rotational speed, and electromagnetic torque. The SOS-based optimally tuned parameters of the TCSC and PSS under severe disturbances were robust and effective, and they enhanced different responses of the system and showed better performance than the other two algorithms in treating different perturbations. The improvement associated with the SOS-based PSS is due to the fact that the SOS algorithm leads to a better near-global solution of the optimization problem under study. The results presented in this paper demonstrated that the computation time associated with the SOS algorithm to reach a better near-global solution was much smaller than the computational times of the other two optimization algorithms.

References

[1] Kundur P. Power System Stability and Control. New York, NY, USA: McGraw-Hill, 1994.

[2] Larsen EV, Swann DA. Applying power system stabilizers part I: general concepts. IEEE T Power Ap Syst 1981; 100: 3017-3024.

[3] Bhattacharya K, Nanda J, Kothari ML. Optimization and performance analysis of conventional power system stabilizers. Int J Elec Power 1997; 19: 449-458.

[4] Hariri A, Malik OP. A fuzzy logic based power system stabilizer with learning ability. IEEE T Energy Conver 1996; 11: 721-727.

[5] Segal R, Kothari ML, Madnani S. Radial basis function (RBF) network adaptive power system stabilizer. IEEE T Power Syst 2000; 15: 722-727.

[6] Abido MA. Robust design of multi-machine power system stabilizers using simulated annealing. IEEE T Energy Conver 2000; 15: 297-304.

[7] Do Bomfim ALB, Taranto GN, Falcao DM. Simultaneous tuning of power system damping controllers using genetic algorithms. IEEE T Power Syst 2000; 15: 163-169.

[8] Abido MA, Abdel-Magid YL. Optimal design of power system stabilizers using evolutionary programming. IEEE T Energy Conver 2002; 17: 429-436.

[9] Abido MA. Optimal design of power-system stabilizers using particle swarm optimization. IEEE T Energy Conver 2002; 17: 406-413.

[10] Zhao Q, Jian J. Robust controller design for generator excitation systems. IEEE T Energy Conver 1995; 10: 201-209.

[11] Chen GP, Malik OP, Qin YH, Xu GY. Optimization technique for the design of a linear optimal power system stabilizer. IEEE T Energy Conver 1992; 7: 453-459.

[12] Hossenizadeh N, Kalam A. A rule based fuzzy power system stabilizer tuned by a neural network. IEEE T Energy Conver 1999; 14: 773-779.

[13] Hingoran NG, Gyugyi L. Understanding FACTS Concepts and Technology of Flexible AC Transmission Systems. New Jersey, NJ, USA: Wiley-IEEE Press, 2000.

[14] Noroozian M, Angquist L, Ghandhari M, Anderson G. Improving power system dynamics by series-connected FACTS devices. IEEE T Power Deliver 1997; 12: 1635-1641.

[15] Paserba JJ, Miller NW, Larsen EV, Piwko RJ. A thyristor controlled series compensation model for power system stability analysis. IEEE T Power Delıver 1995; 10: 1471-1478.

[16] Del Rosso AD, Canizares CA, Dona VM. A study of TCSC controller design for power system stability improvement. IEEE T Power Syst 2003; 18: 1487-1496.

[17] Panda S, Patel RN, Padhy NP. Power system stability improvement by TCSC controller employing a multi-objective genetic algorithm approach. Int J Int Tech 2006; 1: 266-273.

[18] Panda S, Padhy NP. Thyristor controlled series compensator based controller design employing genetic algorithm: a comparative study. Int J Electr Circ Syst 2007; 1: 38-47.

[19] Abido MA. Pole placement technique for PSS and TCSC-based stabilizer design using simulated annealing. Electr Pow Syst Res 2000; 22: 543-554.

[20] Abdel-Magid YL, Abido MA. Robust coordinated design of excitation and TCSC-based stabilizers using genetic algorithms. Electr Pow Syst Res 2004; 69: 129-141.

[21] Panda S, Padhy NP. Coordinated design of TCSC controller and PSS employing particle swarm optimization technique. World Acad Sci Eng Technol 2007; 4: 427-435.

[22] Narne R, Panda P, Therattil JP. Transient stability enhancement of SMIB system using PSS and TCSC-based controllers. In: 2011 IEEE Ninth International Conference on Power Electronics and Drive Systems; 5–8 December 2011; Singapore. New York, NY, USA: IEEE.

[23] Theja BS, Rajasekhar A, Abraham A. An optimal design of coordinated PI based PSS with TCSC controller using modified teaching learning based optimization. In: 2013 World Congress on Nature and Biologically Inspired Computing; 12–14 August 2013, Fargo, ND, USA. New York, NY, USA: IEEE.

[24] Hadi SP, Wiennetou HI, Mochamad RF. TCSC power oscillation damping and PSS design using genetic algorithm modal optimal control. Int J Eng Comp Sci 2013; 13: 23-30.

[25] Rezazadeh A, Sedighizadeh M, Hasaninia A. Coordination of PSS and TCSC controller using modified particle swarm optimization algorithm to improve power system dynamic performance. J Zhejiang Univ-SC C 2010; 11: 645-653.

[26] Khorram AB, Lesani BH, Haghifam CM. Design coordinated controller PSS and TCSC for power dampıng oscillations using bacterial foraging algorithm. International Journal of Advance Technology and Engineering Research 2013; 3: 1-8.

[27] Jalilzadeh S, Noroozian R, Tirtashi MRS, Farhang P. Comparison of TCSC and PSS state feedback controller performances on damping of power system oscillations using PSO. In: 2011 19th Iranian Conference on Electrical Engineering; 17–19 May 2011; Tehran, Iran. New York, NY, USA: IEEE.

[28] Naresh G, Raju MR, Narasimham SVL. Coordinated design of power system stabilizers and TCSC employing improved harmony search algorithm. Swarm Evol Comput 2016; 27: 169-179.

[29] Ali ES, Abd-Elazim SM. Coordinated design of PSSs and TCSC via bacterial swarm optimization algorithm in a multimachine power system. Int J Elec Power 2012; 36: 84-92.

[30] Davarani RZ, Ghazi R. Optimal simultaneous coordination of PSS and TCSC using multi objective genetic algorithm. J Electr Syst 2013; 9: 410-421.

[31] Cheng MY, Prayogo D. Symbiotic organisms search: a new metaheuristic optimization algorithm. Comput Struct 2014; 139: 98-112.

[32] Guvenc U, Duman S, Dosoglu MK, Kahraman HT, Sonmez Y, Yılmaz C. Application of symbiotic organisms search algorithm to solve various economic load dispatch problems. In: 2016 International Symposium on Innovations in Intelligent Systems and Applications (INISTA); 2–5 August 2016; Sinaia, Romania. New York, NY, USA: IEEE.

[33] Kahraman HT, Dosoglu MK, Guvenc U, Duman S, Sonmez Y. Optimal scheduling of short-term hydrothermal generation using symbiotic organisms search algorithm. In: 2016 4th International İstanbul Smart Grid Congress and Fair; 20–21 April 2016; İstanbul, Turkey. New York, NY, USA: IEEE.

[34] Dosoglu MK, Guvenc U, Duman S, Sonmez Y, Kahraman HT. Symbiotic organisms search optimization algorithm for economic/emission dispatch problem in power systems. Neural Comput Appl (in press).

[35] Sonmez Y, Kahraman HT, Dosoglu MK, Guvenc U, Duman S. Symbiotic organisms search algorithm for dynamic economic dispatch with valve-point effects. J Exp Theor Artif In 2017; 29: 495-515.

[36] Dorf RC, Bishop RH. Modern Control Systems. 9th ed. Upper Saddle River, NJ, USA: Prentice Hall, 2001.

[37] Wright A. Genetic algorithms for real parameters optimization. In: Rawlines JE, editor. Foundations of Genetic Algorithms. San Mateo, CA, USA: Morgan Kaufmann, 1991. pp. 205-218.

[38] Kennedy J, Eberhart RC. Particle swarm optimization. In: IEEE International Conference on Neural Networks; 27 November–1 December 1995; Perth, Australia. Piscataway, NJ, USA: IEEE. pp. 1942-1948.

[39] Panda S, Padhy NP. Comparison of particle swarm optimization and genetic algorithm for FACTS-based controller design. Appl Soft Comput 2008; 8: 1418-1427.